Fatigue performance of copper and copper alloys before and after irradiation with fission neutrons

Singh, B.N.; Stubbins, J.F.; Toft, P.

Publication date:
1997

Document Version
Publisher's PDF, also known as Version of record

RISØ

DK9700117

Risø-R-991(EN)

Fatigue Performance of Copper and Copper alloys before and after Irradiation with Fission Neutrons

(ITER R & D Task No. T213)

B.N. Singh[1], J.F. Stubbins[2] and P. Toft[1]

[1]Materials Department
Risø National Laboratory
Roskilde, Denmark

and

[2]Department of Nuclear Engineering
University of Illinois
Urbana, Illinois, USA

Risø National Laboratory, Roskilde, Denmark
May 1997

SOME PAGES ARE MISSING

IN THE ORIGINAL DOCUMENT

Fatigue Performance of Copper and Copper alloys before and after Irradiation with Fission Neutrons

Risø-R-991(EN)

(ITER R & D Task No. T213)

B.N. Singh[1], J.F. Stubbins[2] and P. Toft[1]

[1]Materials Department
Risø National Laboratory
Roskilde, Denmark

and

[2]Department of Nuclear Engineering
University of Illinois
Urbana, Illinois, USA

Risø National Laboratory, Roskilde, Denmark
May 1997

Abstract The fatigue performance of pure copper of the oxygen free, high conductivity (OFHC) grade and two copper alloys (CuCrZr and CuAl-25) was investigated. Mechanical testing and microstructural analysis were carried out to establish the fatigue life of these materials in the unirradiated and irradiated states. The present report provides the first information on the ability of these copper alloys to perform under cyclic loading conditions when they have undergone significant irradiation exposure. Fatigue specimens of OFHC-Cu, CuCrZr and CuAl-25 were irradiated with fission neutrons in the DR-3 reactor at Risø with a flux of ~2.5 × 10^{17} n/m^2s (E > 1 MeV) to fluence levels of 1.5 - 2.5 × 10^{24} n/m^2s (E >1 MeV) at ~47 and 100°C. Specimens irradiated at 47°C were fatigue tested at 22°C, whereas those irradiated at 100°C were tested at the irradiation temperature.

The major conclusion of the present work is that although irradiation causes significant hardening of copper and copper alloys, it does not appear to be a problem for the fatigue life of these materials. In fact, the present experimental results clearly demonstrate that the fatigue performance of the irradiated CuAl-25 alloy is considerably better in the irradiated than that in the unirradiated state tested both at 22 and 100°C. This improvement, however, is not so significant in the case of the irradiated OFHC-copper and CuCrZr alloy tested at 22°C.These conclusions are supported by the microstructural observations and cyclic hardening experiments.

ISBN 87-550-2313-4
ISSN 0106-2840

Information Service Department, Risø, 1997

Contents

1 Introduction

The ITER design conditions require the use of high thermal conductivity materials for high heat sink applications in first wall, limiter and divertor components. Copper alloys provide the best potential to meet the requirement for high thermal conductivity in these applications. There has been a concerted effort, now spanning more than ten years, to identify acceptable copper alloys which can both meet the high thermal conductivity requirements and withstand the temperature, stress and irradiation exposure to which they will be subjected in ITER components. A number of studies of several aspects of copper alloy performance, has led to the primary consideration of three copper alloys for extensive testing and possible development. These alloys include one dispersion strengthened (DS) alloy, Glidcop CuAl25, and two precipitation hardened (PH) alloys: CuCrZr and CuNiBe. Each of these three alloys has specific advantages for application, and certain drawbacks which might either limit or completely prohibit its use. On the basis of currently available data, the dispersion strengthened CuAl-25 alloy is being considered as the primary candidate alloy. Screening experiments are being carried out to select a backup alloy [1,2].

The fatigue behavior is central to materials selection since the vacuum vessel components in ITER will be subjected to thermal cycling, and thus thermal-mechanical cycling, as a result of the cyclic plasma burn operation of the system. This requires that materials can withstand larger numbers of thermal-mechanical loading cycles in order to meet reasonable component lifetime requirements. While the divertor components are replaceable, first wall and limiter tiles are intended to remain sound for the life of the system. In either case, the component design lifetime is set by it resistance to fatigue. These components must also be able to withstand large disruptions without failure. These large transients should be infrequent during the service life, but indicate the need to establish low cycle fatigue performance for very disruptive events which may occur on the order of hundreds or thousands of times during the component life, rather than the several hundreds of thousand cycles incurred during normal operation. These design requirements set the limits of useful fatigue testing in range between around 10 to around 10^6 cycles to failure.

In view of these requirements, an experimental programme was initiated to examine the fatigue behaviour of copper and copper alloys in the unirradiated and irradiated conditions. The fatigue performance of these materials in the unirradiated condition at room temperature has been reported earlier [3,4]. The present work examines the fatigue behaviour of OFHC-Cu, CuCrZr and CuAl-25 in the unirradiated and irradiated conditions at room temperature and 100°C. It should be pointed out that the effect of irradiation on the low cycle fatigue behaviour of these materials is not available in the literature and the present work is the first in this area. The significance of the present results is discussed in terms of the effect of irradiation on dislocation generation and the effect of particles on the motion of dislocations generated during fatigue. The role of mobile dislocatoins in removing the irradiation-induced defect clusters is also considered.

2 Materials and Experimental Procedure

The materials used in the present investigations were oxygen free high conductivity (OFHC) copper, precipitation hardened CuCrZr and dispersion strengthened Glid Cop™ CuAl-25 (LOCL). The OFHC-Cu and CuCrZr were supplied by Tréfimétaux (France) in the form of 20 mm thick plates. The Glid Cop™ CuAl-25 (LOCL), hence forth referred to as CuAl-25, was supplied by OGM Americas (formerly SCM Metals Inc.) in the form of 15 and 20 mm diameter rods in the as-extruded (i.e. wrought) condition. The chemical composition of these materials is listed in Table 1 and the thermomechanical treatments given to these materials prior to testing and irradiations are described in Table 2.

Table 1. Chemical Composition

OFHC-Cu:	Cu - 10, 3 < 1 and < 1 ppm of Ag, Si, Fe, and Mg, respectively
CuCrZr:	Cu - 0,8% Cr, 0.07% Zr, 0.01% Si
CuAl-25	Cu - 0.25% Al as oxide particles (0.46% Al_2O_3)

Table 2. Thermomechanical Treatments

OFHC-Cu:	Annealed at 550°C for 2 h in vacuum (< 1.33 MPa)
CuCrZr:	Solution annealed at 975°C for 30 min. in vacuum (< 1.33 Mpa), water quenched, aged at 475°C for 30 min. in vacuum (< 1.33 Mpa) and water quenched
CuAl-25	As-supplied, i.e. as wrought, no subsequent heat treatment

The subsize fatigue specimens (see Figure 1) of OFHC-Cu, CuCrZr and CuAl-25 were irradiated with fission neutrons in the DR-3 reactor at Risø at the reactor ambient temperature (~47°C) and 100°C. All specimens were irradiated with a neutron flux of ~2.5×10^{17} n/m^{2}s (E > 1 MeV) which corresponds to a displacement damage rate of ~5×10^{-8} dpa(NRT)/s. The OFHC-Cu specimens received a fluence of ~2.5×10^{24} n/m^2 (E > 1 MeV) corresponding to a displacement dose level of ~0.5 dpa. Specimens of CuCrZr and CuAl-25 received a fluence of ~1.5×10^{24} n/m^2 (E > 1 MeV) corresponding to a displacement dose level of ~0.3 dpa.

Mechanical testing was carried out in an Instron machine with a specially constructed vacuum chamber where subsized fatigue specimens could be gripped and loaded. Fatigue tests were conducted primarily in a load controlled mode in an servo-electrical mechanical test stand. The characteristics of the loading cycle were monitored and controlled by computer. The loading cycles were always fully reversed (i.e. R = -1) so that the maximum tension load was the same as the maximum compressive load. The loading frequency was typically 0.5 Hz. The specimens tested in fatigue were cycled to failure, where failure was defined as separation of the specimen into to halves.

For elevated temperature testing, the specimens were heated by electrical resistance furnaces such that the heat was conducted through the specimen grips.

This resulted in accurate temperature control and no measurable temperature gradient along the specimen length.

In addition to the cyclic fatigue tests, a number of cyclic step-loading tests were carried out to establish the cyclic stress-strain response of unirradiated and irradiated materials. These tests were conducted in strain control and the load was continuously monitored and recorded for the duration of each test. The tests provided an indication of the stress-strain response of the material under cyclic loading conditions. The resulting cyclic stress-strain curves are useful for interpreting the respective material hardening or softening behaviour under fatigue loading conditions.

Following fatigue of both unirradiated and irradiated materials, fracture surfaces were examined in a JEOL 5310 low vacuum scanning electron microscope (SEM). For transmission electron microscopy investigations, 3 mm discs were cut from the gauge sections (close to the fracture surface) perpenticular to the fatigue axis. The discs were mechanically thinned to ~0.1 mm and then twin-jet electropolished in a solution of 25% perchloric acid, 25% ethanol and 50% water at 11 V for about 15 seconds at ~20°C. The thin foils were examined in a JEOL 2000 FX transmission electron microscope.

3 Experimental Results

3.1 Pre- and Post-irradiation Microstructure

In order to understand the cyclic deformation behaviour of these materials, it is important to know the details of the pre-fatigue microstructure before and after irradiation. Figure 2 shows optical micrographs of the OFHC-Cu and CuCrZr after the heat treatment specified in Table 2. The average grain size was found to be about 100 μm both for OFHC-Cu and CuCrZr . The CuAl-25 has a grain size of < 1 μm which is too small to reliably measure using optical metallography. Figure 2 (c) shows the grain structure of CuAl-25 taken in a transmission electron microscope (TEM) [1]. The dislocation density in OFHC-copper and CuCrZr is found to be rather low (< 10^{12} m^{-2}) [5]. In contrast, the CuAl-25 alloy in the as-wrought condition was found to contain a dislocation density of 1.5×10^{15} m^{-2} [5]. Most of these dislocations were associated with alumina particles.

The microstructure of the prime aged and unirradiated CuCrZr was dominated by the high density (1.5×10^{23} m^{-3}) of coherent platelets and small spherical precipitates [5]. The spatial distribution of these precipitates was fairly homogeneous. The density of alumina particles in the CuAl-25 alloy was significantly lower (2.2×10^{22} m^{-3}) than that in the CuCrZr alloy. On the other hand, the alumina particles were considerably larger in size [~8.7 nm in diameter) than the precipitates in the CuCrZr alloy. It should be pointed out here that the spatial distribution of alumina particles was found to be very heterogeneous; both particle size and density varied very considerably [1, 5].

The main effect of irradiation with fission neutrons at ~47°C was the introduction of interstitial and vacancy type defect clusters in high densities. A cluster density of ~5×10^{23} m^{-3} was found in OFHC-Cu, CuCrZr and CuAl-25 irradiated with fission neutrons at ~47° C to a dose level of 0.2 dpa [5].

3.2 Fatigue Life Evaluation

The fatigue life test results are shown in Figures 3 through 7 for the three materials used in this study.

The fatigue performance of OFHC-Cu is indicated in Figure 3 for unirradiated and 50°C irradiated specimens; both types of specimens were tested at room temperature. The results presented in Figure 3 tend to suggest that the fatigue life of the irradiated specimens of OFHC-Cu may be longer than that of the unirradiated specimens at stress amplitudes lower than ~150 MPa (i.e. at $N_f > 10^3$ cycles). However, in view of the limited number of results, this trend must be taken to be only tentative in nature. The comparison is further complicated by the fact that while unirradiated specimens are tested in the strain controlled mode, all irradiated specimens are tested in the stress controlled fashion. It should be noted that the stress and the strain controlled tests tend to yield similar results, particularly at lower cycles to failure. However, there are not enough results to confirm this trend.

Figure 4 shows the fatigue life results for CuCrZr irradiated at 50°C and tested at 22°C. The results of the irradiated specimens are similar to that of the fatigue performance of this material in the unirradiated condition over the entire range of loads investigated, from less than 100 cycles to failure to over 10^5 cycles to failure.

The fatigue responses of CuAl-25 shown in Figure 6, indicate a clear improvement in fatigue lives following irradiation to 0.3 dpa at 50°C as compared to the unirradiated condition. For most of the lives greater than about 500 cycles to failure, a modest increase in fatigue life over the unirradiated conditions is found. The slopes of the fatigue curves appear to be nearly parallel in this region, but indicate about a factor of two increase in life for fixed load conditions. At short lives, the irradiated condition has a larger margin of life over the unirradiated conditions. A comparison of the strain controlled and load controlled fatigue lives are also shown in Figure 6 for unirradiated CuAl-25. The two sets of data match very closely. This indicates that the current load controlled tests are directly comparable to strain controlled tests; this issue will be addressed in more detail later. In contrast to the CuCrZr results but consistent with its own room temperature results, the CuAl-25 material shows an improvement in fatigue performance following irradiation and testing at 100°C (Figure 7). In some cases, an improvement of nearly a factor of ten in fatigue lives at a fixed loading condition are found for the CuAl25 in fatigue lives following irradiation to 0.3 dpa (Figure 7).

A comparison of all of the fatigue results shown in Figures 3 through 7 indicates that, for fixed loads, CuAl-25 provides the best fatigue performance at a fixed load, and OFHC-Cu the worst.

3.3 Cyclic Stress-Strain Evaluation

In order to provide useful information regarding the cyclic hardening or softening behaviour of the various alloys and to better correlate the results of stress-controlled and strain-controlled fatigue tests, a series of cyclic stress-strain curves were generated with cyclic step tests. In these tests, fully reversed fatigue loading was carried out at an initially low applied strain level, one in the elastic range. The specimen was cycled for a minimum of twenty cycles at the fixed strain range. The strain range was then increased by a small increment, and at least twenty cycles of loading were applied at each strain level while the load was monitored and recorded. Following stable or nearly stable cycling at each

strain range, the strain range was increased by a small increment and the process repeated. Where possible, these tests were performed by first increasing the strain range incrementally to up to about 2% total strain and then decreasing the strain ranges back down in small increments to very low (i.e. elastic) strain ranges. This allowed for an analysis of residual hardening or softening which can take place during the loading cycles. Tests were performed on both unirradiated and irradiated materials. Examples of the cyclic stress-strain curves for OFHC-Cu are shown in Fig. 8. Figure 8 shows the cycle by cycle softening behavior for loading conditions in the upper yield area on an irradiated specimen of CuCrZr alloy. It should be noted that the material is gradually softening during each loading cycle at any given applied strain range. Thus the final stress level at any given strain depends on the total number of cycles at that condition. The amount of softening per cycle at each strain level, however, does seem to decay to smaller values as the number of cycles increases. In any case, the tendency to cyclically soften is clear in all of the irradiated conditions.

The results of these tests are shown in Figures 9 through 11 for OFHC-Cu, CuCrZr and CuAl-25, respectively. These tests were carried out at room temperature. It can be noted that in all cases the irradiated materials exhibit a higher cyclic "yield" point than do any of the unirradiated materials. In addition, there is an apparent upper and lower yield phenomenon similar to those seen in the monotonic tensile behaviour of the irradiated specimens [5].

Following the initial post-yield drop in cyclic strength in the irradiated conditions, the balance of the cyclic stress-strain curves remain relatively flat, but at much reduced stress levels compared to the initial irradiation-hardened case. This post-yield drop in the cyclic strength is a clear indication of the softening effect induced by defect cluster removal by dislocation sweeping and localized deformation. In the cases of both of the alloys, a somewhat elevated strength persists as compared to the unirradiated curves. In the case of OFHC-Cu (Figure 9), however, once the cyclic softening is induced, the curve very closely follows that of the unirradiated case. In other words, after the initial yield drop the OFHC-Cu shows clear evidence of work hardening. This is a significantly different behaviour compared to the commonly observed behaviour of irradiated copper during tensile tests where plastic instability follows the yield drop and the material looses its ability to work harden [5-7].

The work reported here is based primarily on tests conducted under load control where the specimen is cycled between fixed load limits. It is more common, where possible, to conduct low cycle fatigue tests in the strain controlled mode, where the specimen is cycled between fixed strain (extension) limits. The current work indicates, however, that similar results are obtained from both test methods. When life versus stress amplitude is compared in the current results (see Figures 3 and 6), the results are the same. In order to make the load controlled results more compatible and of broader use, the cyclic stress-strain curves are used to determine the cyclic hardening curves. Figures 12 and 13 show the plastic portions of the stress-strain curves where stress and strain are plotted on a log-log scale. This is shown for OFHC-Cu and for CuAl-25 and results from monotonic tensile test from the same materials are shown. The irradiated and unirradiated behaviours are both included in the analyses. The total cyclic strain can be represented as:

$$\Delta\varepsilon_{total} = \Delta\varepsilon_{elastic} + \Delta\varepsilon_{plastic} = \Delta\sigma / E + (\Delta\sigma / K')^{1/n'}$$

This formulation assumes the standard Ramberg-Osgood-type relationship for strain hardening in the plastic regime, where K' is the cyclic strength coeffi-

cient and n′ is the cyclic hardening exponent. The original formulation was applied to strain hardening under monotonic loading conditions such that

$$\Delta\varepsilon_{total} = \Delta\varepsilon_{elastic} + \Delta\varepsilon_{plastic} = \sigma / E + (\sigma / K)^{1/n}$$

where K is the strength coefficient and n is the strain hardening exponent. These relationships, while empirical, provide an excellent representation of the material deformation behaviour from the elastic regime through a large portion of the post-yield response for a wide variety of metals and alloys. These relationships provide a useful constitutive relationship where the applied stress, or stress amplitude, at any point in the loading can be directly correlated with a unique strain or strain range. Once the constants in either equation have been determined, it is straightforward to convert stresses (or loads) to strain and vice versa.

In the current study, the cyclic stress strain curve provide the means for determining the relevant constants. The stress (or load) based fatigue life curves can be converted to strain-based information using the above equation once the vaues of the constants have been determined. The values of the current constants are shown in the respective figures (Figures 12 and 13). In the simplest case, that is the case, where the stresses are all elastic, the elastic modulus, E, can be used to convert stress to strain. For more complicated cases, where significant plasticity is involved, the entire equation must be used. Figures 14 and 15 show the elastic strain range only, and cyclic hardening results for converting the load controlled tests to strain versus life curves. The conversions are compared to previous strain-controlled tests.

Figures 14 and 15 indicate the viability of converting fatigue performance based on load (stress) controlled tests to the more common strain-life representation. This is accomplished in the current work by either using strains calculated from the elastic modulus, E, or strain calculated from the plastic strain hardenng coefficient, K or K′, and the strain hardening exponent, n or n′. These values are extracted from the Ramburg-Osgood relationships shown in Figures 12 and 13. The conversion of stress or load controlled fatigue life information to a strain-based representation is straight forward for many data in the high cycle fatigue regime where the stresses and strains are predominantly in the elastic regime. When the elastic stress-strain relationship dominates, the strain-based strain vs. life representation is the same as the somewhat antiquated S-N representation where the fatigue life is plotted directly against the applied stress amplitude. Since the stress and strain have a simple, linear relationship in this regime, they are easily converted. This accounts for the high degree of correlation of the curve **labeled** "total strain based on the elastic modulus, irradiated, stress control" in Figures 14 and 15 with the elastic strain portions of the fatigue curves. At very high fatigue lives, greater than 10^5 cycles to failure, the correlation with the total fatigue life is also very good.

The fatigue lives for both OFHC-Cu and CuAl-25 contain a large contribution of plastic strain at intermediate and short lives as indicated in Figures 14 and 15. In order to fully capture the contribution of the plastic strain, the cyclic strength coefficient, K′, and the strain hardening exponen, n′, are usd to convert the stress levels in the load controlled tests to equivalent strains. (It should be noted that the fitting technique also embeds some of the elastic strain information in the relationship as used here). When the stresses from the load controlled tests are converted to equivalent total strain range and plotted against fatigue life, the curves **labeled** "total strain based on plastic hardening, irradiated, stress control" are generated. For OFHC-Cu, the correlations of the irradiated tests with the unirradiated tests over the range of test conditions studied

here is commendable. The correlation is less exact in the high cycle fatigue range where the elastic contribution dominates, as would be expected.

The case of CuAl-25 is somewhat more complicated. The comparisons are not as satisfactory as for the case of OFHC-Cu. Also, contrary to the case of OFHC-Cu, the CuAl-25 fatigue lives following irradiation were rather longer than those of the unirradiated material. When the conversion from stress control to strain range is made, either with the elastic modulus in one case or with the cyclic strength coefficient and cyclic hardening exponent in the other, the predicted fatigue behaviour underperforms that of the unirradiated material. It should also be noted here, that most of the fatigue life data fall into the regime where both the elastic and plastic strain contributions are important. The elastic strain predictions are close to the elastic portion of the strain range, whereas the plastic or cyclic hardening conversions lie substantially above the actual plastic strain curve, but marginally below the actual total strain-life curve for unirradiated material. This indicates that some caution must be taken in this case, at least, when converting from fatigue life data taken from stress controlled tests to strain-based formulations.

3.4 Post-Fatigue Microstructural Characterization

Since neutron irradiation causes a drastic decrease in the uniform elongation of copper and copper alloys [5-7], the possibility that the neutron irradiation may also impair the fatigue performance of these materials cannot be ruled out. The present results strongly suggest, however, that this may not be the case. In fact, the results for the CuAl-25 alloy show just the opposite in that the irradiation improves the fatigue lifetime both at room temperature and 100°C when tested in the post-irradiation condition. In order to understand as to how this improvement occurs, it is necessary to investigate the details of the microstructural evolution during cyclic loading of these materials in the unirradiated and irradiated conditions. For this purpose, a number of specimens of the unirradiated and irradiated OFHC-Cu and CuAl-25 were examined in TEM following fatigue loading. The main observations are summarized in Tables 3 and 4, respectively, for OFHC-Cu and CuAl-25 specimens fatigue tested at room temperature.

The post-fatigue microstructure of OFHC-Cu tested at room temperature in the unirradiated condition is dominated by equiaxed and elongated cells (Figure 16). At the high load level (180 MPa, N_f = 1121) the cell formation occurs throughout the whole specimen. However, the cell formation occurs in an inhomogeneous fashion in that the cells in some areas are equiaxed (Figure 16a) and in other areas narrow and elongated (Figure 16b). At the low load level of 120 MPa (N_L = 21646), most of the cells are narrow and elongated (Figure 16c), but some areas of the specimen contain loose dislocation walls and very long cells.

The microstructural evolution in the irradiated specimens of OFHC-Cu during fatigue testing is found to be substantially differrent from that observed in the unirradiated OFHC-Cu. The post-fatigue microstructure in the irradiated specimens is rather complex and varies significantly with the stress amplitude. Figures 17 through 21 illustrate different features of the post-fatigue microstructure for stress amplitudes from 250 MPa to 80 MPa. At the highest stress amplitude of 250 MPa (N_f = 32), the microstructure is found to contain small cells with loose dislocation walls (Figure 17a), slip bands (Figure 17b) and "cleared" channels (Figure 17c). It can be clearly seen that the interior of the cells and the slip bands (Figures 17a,b) contain very few or no defect clusters

produced during irradiation. A clear example of a "cleared" channel is shown in Figure 17c. It should be noted here that in the regions away from the cleared channel there is no evidence of dislocation generation during the cyclic deformation even at the stress level of 250 Mpa. This is consistent with the lack of dislocation generation in the irradiated OFHC-Cu tensile tested at room temperature [5].

Figure 18 shows the microstructure observed in the irradiated specimens of OFHC-Cu following cyclic deformation at a stress amplitude of 200 MPa (N_f = 424). A mixture of equiaxed and elongated cells can be seen in Figure 18(a). Again, the cells contain very few or no defect clusters. The evidence of cleared channel formation can be seen in Figure 18(b).

The fatigue-induced microstructure of irradiated OFHC-Cu tested at a stress amplitude of 160 MPa (N_f = 1604) is shown in Figure 19. At this stress level, although there is a tendency towards cell formation (Figure 19a), but the formation of proper cells is not completed. The microstructure is dominated, instead, by the fatigue-induced high density of dislocations with a reasonably homogeneous distribution (Figure 19b). As can be seen in Figure 19b, there is a tendency for dislocations to segregate in the form of loose bands. It is significant that at the stress amplitudes of 160 MPa and below, elongated cells and very long dislocation walls or veins are not formed. This would suggest that both generation and the mobility of dislocations are seriously reduced in the irradiated materials.

At the stress amplitude of 80 MPa, there is no indication of formation of cells and subgrains (Figures 20 and 21). However, as can be seen in Figures 20 and 21, dislocations have a tendency to cluster, segregate and form bands of dislocations (Figure 21).

The post-fatigue microstructures of the CuAl-25 alloy in the unirradiated and irradiated conditions are shown in Figures 22 through 24 and the main features are summarized in Table 4. The most significant aspect of these observations is that the overall activities of dislocation (generation, interactions and segregation) is drastically reduced in CuAl-25 compared to that in the OFHC-Cu. At the stress amplitude of 440 MPa (N_f = 262), there is a tendency to form some very small (100 - 200 nm diameter) and rather loose cells (Fig. 22a) in some parts of the specimens. Generally, the microstructure is dominated by the presence of small dislocation segments pinned probably by the oxide particles (Figure 22b). No indication of cell formation was observed in the unirradiated CuAl-25 fatigue tested at a stress amplitude of 360 MPa (Fig. 23). Figure 24 shows the dislocation microstructure of the irradiated CuAl-25 after fatigue testing at stress amplitudes of 540 MPa (Figure 24a) and 320 MPa (Figure 24b). No indication of cell formation was observed in these specimens. In the specimen tested at 320 MPa not all the grains seem to have deformed plastically; a large number of grains still contain as-irradiated cluster and dislocation microstructures. The lack of dislocation generation during the fatigue experiment at 320 MPa can be seen in Figure 24(b).

Table 3. Comparison of Microstructural Observations in Fatigue Tested (at Room Temperature) OFHC-Cu with and without Irradiation Exposure

Unirradiated			Irradiated (47°C, 0.5 dpa)		
N_f	σ (MPa)	Microstructure	N_f	σ (MPa)	Microstructure
1121	180	Mixture of equiaxed and very elongated cells	32	250	Complicated microstructure containing: - small cells with loose dislocation walls - slip bands and "cleared" channels - areas with defect clusters and grown-in dislocations
21646	120	Microstructure dominated by elongated cells - in some cases with loose walls; very elongated cells only in some areas	189	220	Mostly equiaxed cells but some areas contain homogeneous distribution of dislocations
			424	200	Mostly equiaxed cells, however, some areas contains "cleared" channels. Areas were also found where the as-irradiated microstructure had survived and where no dislocations were generated
			1604	160	Tendency to form cells with loose walls, homogeneous distribution of dislocations, clusters appear to have been wiped out
			515988	80	No sign of extensive global plastic deformation, defect clusters are seen every-where, bands of dislo-cations, no indication of cell formation

Table 4. Comparison of Microstructural Observations in Fatigue Tested (at Room Temperature) Glidcop CuAl-25 with and without Irradiation Exposure

Unirradiated			Irradiated (47°C, 0.3 dpa)		
N_f	σ (MPa)	Microstructure	N_f	σ (MPa)	Microstructure
262	440	Dislocation generation, interactions and tendency to form small (100-200 nm) loose cells	129	540	High density of homogeneously distributed dislocations, most of the defect clusters appear to have been wiped out or at least cannot be identified
2994	360	Homogeneous distribution of dislocations in the grains	247	500	High dislocation density, tendency to form small (~200 nm) loose cells, defect clusters appear to have been wiped out
			3235	400	Density of dislocations generated by deformation rather low, no indication of cell formation, not all the grains appear to have deformed plastically (these grains still contain as-irradiated defect clusters and dislocation micro-structure)
			49506	320	Only a few grains appear to have deformed plastically and a large number of grains still contain as-irradiated cluster and dislocation microstructure

3.5 Fracture Surface Analysis

The fracture surfaces of the fatigue specimens were examined by SEM to identify significant features which could relate to the fatigue performance. A comparison of the macroscopic features of the unirradiated and irradiated fracture surfaces is shown in Figure 25 for OFHC-Cu and in Figure 26 for CuAl-25. A comparison of the irradiated and unirradiated conditions indicates that, while the fracture surfaces are reasonably flat in the case of unirradiated materials, the irradiated conditions indicate a significant amount of necking during the final stages of fatigue loading. This is thought to be directly related to the cyclic hardening in the unirradiated materials which should not lead to necking, and the cyclic softening in the case of irradiated materials which could lead to necking. This should also be evident from the upper yield point phenomenon shown by the cyclic stress-strain curves for the irradiated materials.

A closer examination of the failure surfaces provides more information regarding the nature of the fractures. A comparison of the unirradiated and irradiated OFHC-Cu fracture surfaces indicates that in the unirradiated condition specimens failed by the classic fatigue crack initiation and growth mechanism. The fatigue striations are clearly evident on the failure surfaces indicating that the crack advanced through the specimen with little redistribution of plasticity. No secondary cracking or other crack branching is evident. On the contrary, the irradiated material shows extensive deformation up to the point of separation (Fig. 25c), which is also a result of ductile fracture. The clear indication of intersection flow lines over all of the materials surface indicates the extent to which plastic deformatin is distributed around the neck region.

By somewhat of a contrast, the failure surfaces of the unirradiated and irradiated CuAl-25 are rather similar. In both cases the evidence of secondary cracking is observed. While necking is seen in the irradiated conditions, the nature of the final fracture surfaces are microscopoically similar. A limited amount of plasticity-induced deformation void formation is apparent and the final failures appear to be relative ductile in nature. The ductility, however, is constrained to this very large population of voids, which appears to be associated with the alumina particle distributions (Fig. 26c).

4 Discussion

The results of the low cycle fatigue experiments carried out on OFHC-Cu, CuCrZr and CuAl-25 both in the unirradiated and irradiated conditions have demonstrated two significant features of the effect of irradiation on their performance. First, the irradiated materials exhibit an yield drop and softening during the first few cycles of fatigue experiments. In the case of irradiated OFHC-Cu, the yield drop is followed by hardening at higher fatigue cycles. Second, the fatigue life of the irradiated materials tested at 22°C is noticeably improved by irradiation (Figures 3, 4, 6, 7). The fact that the effect of irradiation on fatigue life is relatively innocuous or even positive is of academic as well as of technological interest (e.g. for the lifetime of components in ITER). In the following, both of these issues are discussed particularly in terms of the results of microstructural investigations and fracture surface analyses.

Let us first consider the origin and implications of the initial yield drop (cyclic softening) followed by hardening or hardening and plastic instability in

the irradiated OFHC-Cu, CuCrZr and CuAl-25. It is relevant to note here that the initial yield drop is a matter of common observations in copper irradiated and tensile tested at temperatures below the recovery stage V (i.e. <0.3 T_m where T_m is the melting temperature) to a dose level of about 0.1 dpa or higher (e.g. [5 - 7]). The occurrence of a prominent yield drop in a pure fcc metal is, however, highly unusual. Generally, the yield drop is a characteristic deformation feature of the bcc metals containing interstitial impurities (e.g. carbon and nitrogen in iron). It is well established that the impurity atoms segregate at the dislocations and prevent them from acting as Frank-Read sources. At the upper yield stress, a large number of dislocations break away from the atmosphere of the impurity atoms, causing a yield-drop. This is consistent with the theoretical prediction that a prominent yield drop is likely to occur when the density of unlocked dislocation is very low (10^6 - 10^8 m^{-2}) [8]. This clearly suggests that the grown-in dislocations in copper must get locked during irradiation and it is their release at the upper yield stress which causes the yield drop. The question then arises as to how the grown-in dislocations get locked during irradiation?

This question has been addressed recently in a new model for radiation hardening called "Cascade Induced Source Hardening" (CISH) [9]. In this model, the grown-in dislocations are taken to be decorated by small loops of self-interstitial atoms (SIAs). The upper yield stress is the stress necessary to pull the dislocation away from the atmosphere of loops surrounding the grown-in dislocations. It has been further shown that the decoration is caused by the one-dimensional glide of small SIA loops/clusters produced in the cascades [10]. The experimental evidence showing the decoration of grown-in dislocations by SIA loops is reviewed in [10].

Thus, the observed yield drop behaviour in copper and copper alloys can be understood in terms of the CISH model. The fact that the yield-drop in the case of the CuAl-25 alloy is very small can be easily rationalized in terms of the high density of grown-in dislocations (1.5×10^{15} m^{-2} [5]) and the presence of dispersions of hard Al_2O_3 particles acting as strong obstacles to dislocation motion. In the case of CuAl-25, most of the grown-in dislocations (introduced during manufacturing process) are associated with Al_2O_3 particles and thereby strongly locked. During deformation, even if some of the dislocations are unlocked at the upper yield stress, they cannot move long distances because Al_2O_3 particles will block their motion.

In this context, it is worth pointing out that the post-fatigue microstructures observed in the irradiated OFHC-Cu and CuAl-25 provide an overwhelming amount of evidence for a very efficient removal of the irradiation-induced defect clusters by the dislocations generated during the cyclic loading. Once the dislocations are generated, they move under the influence of applied stress and wipe out practically all defect clusters in their path by elastic force field interactions between small loops and gliding dislocations. This implies that the irradiation-induced defect clusters do not act as strong obstacles to the dislocation motion and therefore are unlikely to be the cause of the observed hardening [9]. Instead, the irradiation produced cascades render the generation of dislocations more difficult or impossible by inducing decoration of the grown-in dislocations by small loops. This leads to an increase in the uper yield stress and inhomogeneous and localized deformation and gives rise to yield drop and plastic instability. This explains the observation of prominent necking during cyclic loading of the irradiated OFHC-Cu and CuCrZr. The corresponding unirradiated specimens tested under the same condition, on the other hand, do not exhibit neck formation.

In view of the complicated nature of the deformation processes operating under cyclic loading conditions, it is not possible at present to provide a simple explanation for the observed lack of deleterious effects, and even a positive effect (i.e. increase in lifetime) of irradiation on fatigue lifetime, particularly in the case of the CuAl-25 alloy. It is important to recognize here that while the unirradiated copper and copper alloys deform homogeneously (i.e. without necking), the deformation in the irradiated materials is dominated by localized deformation producing prominent necking (Figures 9, 25, 26). It should be pointed out that the necking is prominent only in the OFHC-Cu and CuCrZr, but not in the case of the irradiated CuAl-25.

This difference in the deformation behaviour between the unirradiated and irradiated states makes the comparison of their lifetime rather questionable. Furthermore, it is reasonable to speculate that the observed yield drop and necking may be due to the fact that fatigue experiments are conducted in the stress-controlled mode. The strain-controlled test, on the other hand, may prevent the localization of deformation and necking. This may yield a longer lifetime. In other words, the stress-controlled fatigue tests may underestimate the lifetime which may be achieved under the condition where the cyclic loading may correspond to the strain controlled experiments (e.g. in the first wall and divertor components in ITER).

The fatigue lifetime improvement exhibited by the irradiated specimens of CuAl-25 both at 22 and 100°C (Figures 6 and 7) is consistent with the line of argument presented above. The irradiated CuAl-25 alloy, for instance, does not suffer from a prominent yield drop and extensive necking and yields a significantly longer lifetime in the whole range of the stress amplitudes used in the present experiments both at 22 and 100°C. It should be pointed out that the irradiated CuAl-25 does not suffer from the yield drop during tensile testing at 22°C [5,7] either.

The post-fatigue microstructural investigations of the irradiated CuAl-25 alloy demonstrate two significant features: (a) difficulty in dislocation generation and (b) the lack of fatigue-damage accumulation in the form of large elongated cells or subgrains. These observations are consistent with the results of the cyclic stress-strain experiments (Figure 11). These results suggest that although the alumina particles in the CuAl-25 alloy are strong obstacles to dislocation motion, the irradiation induced decoration of the grown-in dislocations is still efficient in preventing dislocation generation.

It should be recognized though that this irradiation-induced improvement in the fatigue performance may not occur in the in-situ experiments corresponding to the service conditions of ITER. Under the dynamic conditions of ITER, it may be difficult, or even impossible, to decorate the grown-in dislocations by small SIA loops, because of the low displacement dose per burn-up cycle. In other words, the dislocation generation during the cyclic deformation during irradiation may occur in the same manner as in the case of unirradiated materials. Hence, an improvement in the fatigue lifetime may not occur. On the other hand, since the mobile dislocations under the dynamic conditions will keep removing the defect clusters produced by the cascades, the irradiation may not cause any deleterioius effects on fatigue life either. It may be of interest, therefore, to carry out post-irradiation fatigue experiments on specimens irradiated to low doses (e.g. ~10^{-2} dpa), particularly on CuAl-25 alloy where the positive effect of alumina particles on dislocation generation and motion still may be maintained.

5 Summary and Conclusions

In the present work, the low cycle fatigue behaviour of the annealed OFHC-Cu, prime aged precipitation hardened CuCrZr and dispersion strengthened CuAl-25 has been investigated before and after these materials were exposed to neutron irradiation. All three materials were irradiated at ~47°C and tested at 22°C. In addition, CuCrZr and CuAl-25 alloys were irradiated and tested at 100°C. The unirradiated specimens were tested both in stress- and strain-controlled modes, whereas all irradiated specimens were tested only in the stress-controlled mode. In order to determine the cyclic hardening or softening behaviour of these alloys and to establish a correlation between the results of the stress-controlled and strain-controlled fatigue tests, a series of cyclic stress-strain curves were generated with cyclic step tests. To facilitate a better understanding of the mechanical performance of these materials, the microstructure and fracture surfaces were investigated in detail using transmission and scanning electron microscopes.

On the basis of the results of the mechanical testings and microstructural investigations, the following main conclusions may be drawn:

- The unirradiated specimens tested at 22°C in the stress- and strain-controlled modes exhibits similar fatigue life.
- The cyclic step tests clearly demonstrate that the irradiated specimens of OFHC-Cu and CuCrZr suffer from a prominent yield drop; the irradiated CuAl-25 specimens, on the other hand, do not exhibit such a prominent yield drop.
- All unirradiated specimens deform homogeneously, whereas irradiated specimens of both OFHC-Cu and CuCrZr deform inhomogeneously and exhibit extensive necking during fatigue experiments. The amount of necking observed in the irradiated CuAl-25 specimens is very limited.
- Irradiated specimens of OFHC-Cu, CuCrZr and CuAl-25 exhibit a noticeable improvement in the fatigue performance due to irradiation. This improvement is quite significant in the case of CuAl-25 both at 22 and 100°C.
- The use of cyclic step tests to generate cyclic stress-strain curves is a useful means of comparing the effects of cyclic loading to monotonic (tensile) loading, and to generate cyclic strength coefficient, K', and cyclic hardening exponent, n', which are useful for interpreting load control vs. strain control fatigue life data.
- The data analysis based on cyclic strain hardening behaviour allow for conversion of fatigue life information from load control tests to strain-based correlations. This conversion must be used with some care, however, particularly when trying to compare data from irradiated tests and unirradiated tests which are obtained with different test control conditions. Nevertheless, the information provides useful guidance for interpreting stress controlled test data when design conditionss may require strain-based information.
- The observed post-fatigue microstructures indicate that the difficulty in the generation of fresh dislocations during fatigue deformation limits the scale of the fatigue damage accumulation and may be responsible for the improvement in the observed fatigue lifetime. In the case of CuAl-25, the presence of Al_2O_3 particles make further contribution to this improvement by acting as strong obstacles to dislocation motion.
- The irradiation-induced defect clusters do not appear to act as effective obstacles to dislocation motion during fatigue deformation; once generated, the

mobile dislocations wipe out the irradiation-induced defect clusters. A similar behaviour has been observed in the irradiated and tensile tested specimens of OFHC-Cu.

- The analysis of the present results suggests, however, that the irradiation-induced improvement in the fatigue lifetime observed in the post-irradiation tests may not occur during the service condition of ITER where the accumulated damage in one burn-up cycle may not be high enough to decorate the grown-in dislocations (by small SIA loops) and render them immobile. On the other hand, since the mobile dislocations generated during cyclic deformation are quite effective in removing the irradiation-induced defect clusters, the irradiation may not cause deleterious effects on the fatigue lifetime of these materials.
- It is suggested that the post-irradiation fatigue testing of specimens irradiated to low doses ($\leq 10^{-2}$ dpa) may be useful in verifying the above conclusion, particularly in the case of CuAl-25 alloy.

Acknowledgements

The present work was partly funded by the European Fusion Technology Programme. The authors would like to thank B.F. Olsen and J.L. Lindbo for the technical assistance.

References

[1] B.N. Singh, D.J. Edwards, M. Eldrup and P. Toft, Risø-R-937 (EN), January 1997.

[2] B.N. Singh, D.J. Edwards, M. Eldrup and P. Toft, Risø-R-971 (EN), February 1997.

[3] A. Singhal, J. F. Stubbins, B. N. Singh and F. A. Garner, J. Nucl. Mater. **212-215** (1994) 1307.

[4] K. D. Leedy, J. F. Stubbins, B. N. Singh and F. A. Garner, J. Nucl. Mater. **233-237** (1996) 547.

[5] B.N. Singh, D.J. Edwards and P. Toft, J. Nucl. Mater. **238** (1996) 244.

[6] S.A. Fabritsiev, S.J. Zinkle and B.N.Singh, J. Nucl. Mater. **233-237** (1996) 127.

[7] B.N. Singh, A. Horsewell, P. Toft and D.J. Edwards, J. Nucl. Mater. **224** (1995) 131.

[8] G.T. Hahn, Acta Met. **10** (1962) 727.

[9] B.N. Singh, A.J.E. Foreman and H. Trinkaus, J. Nucl. Mater. (1997), in press.

[10] H. Trinkaus, B.N. Singh and A.J.E. Foreman, J. Nucl. Mater. (1997), in press.

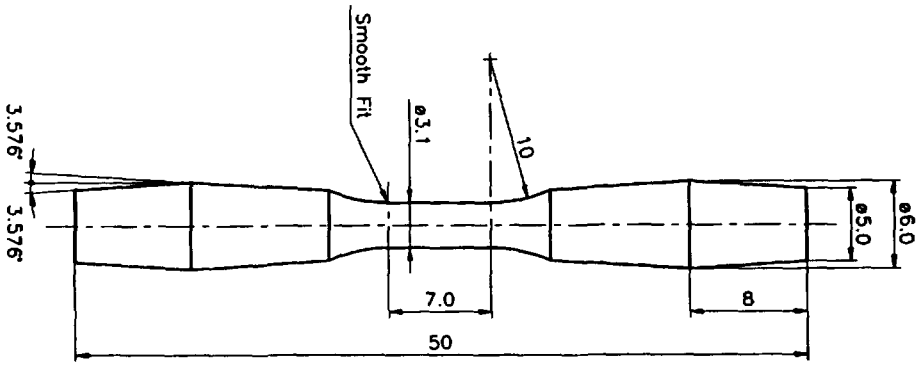

Figure 1. Geometry and dimensions of fatigue specimens.

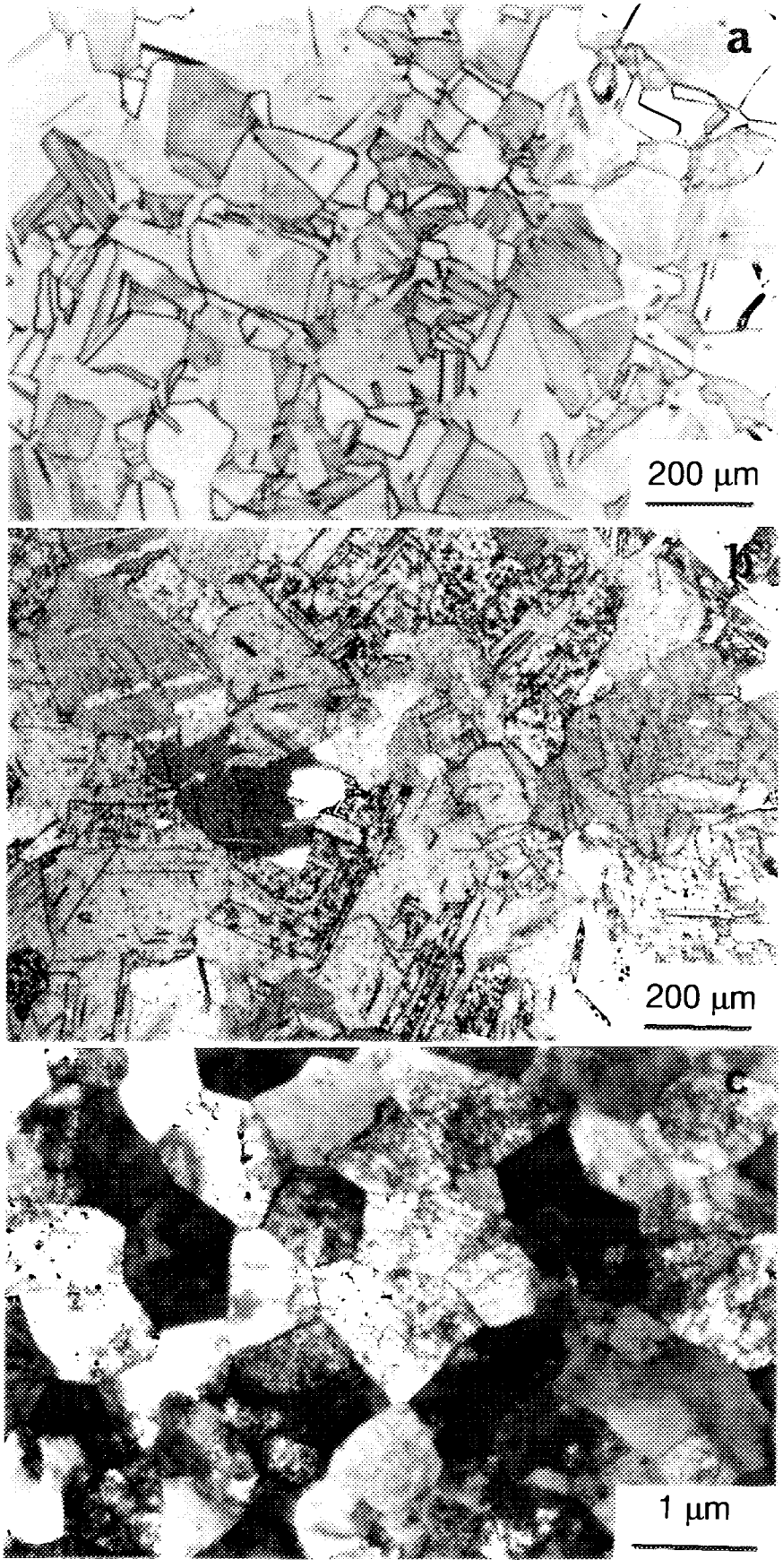

Figure 2. Microstructure of the unirradiated copper and copper alloys: (a) OFHC-Cu (annealed at 550°C for 2 h), (b) CuCrZr (prime aged) and (c) CuAl-25 (as-wrought).

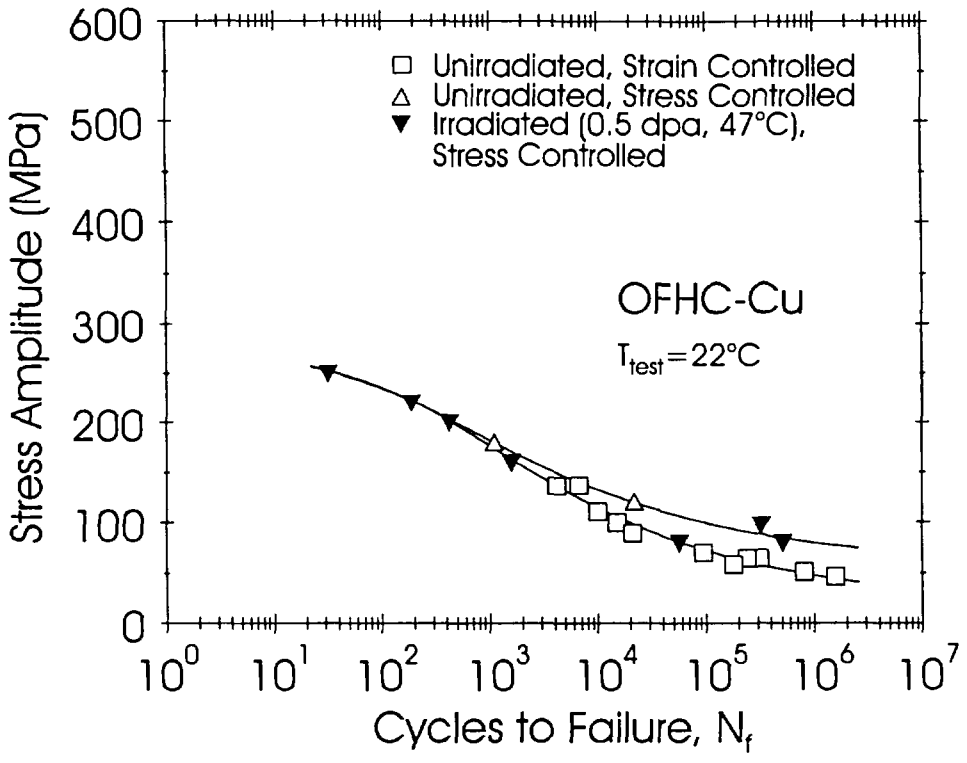

Figure 3. Fatigue life (N_f) as a function of stress amplitude for unirradiated and irradiated OFHC-Cu tested at room temperature in vacuum. Irradiation was carried out at ~47°C to a dose level of ~0.5 dpa (NRT). Note, that both stress- and strain-controlled tests give similar fatigue life, N_f. Furthermore, the fatigue life appears to increase due to irradiation.

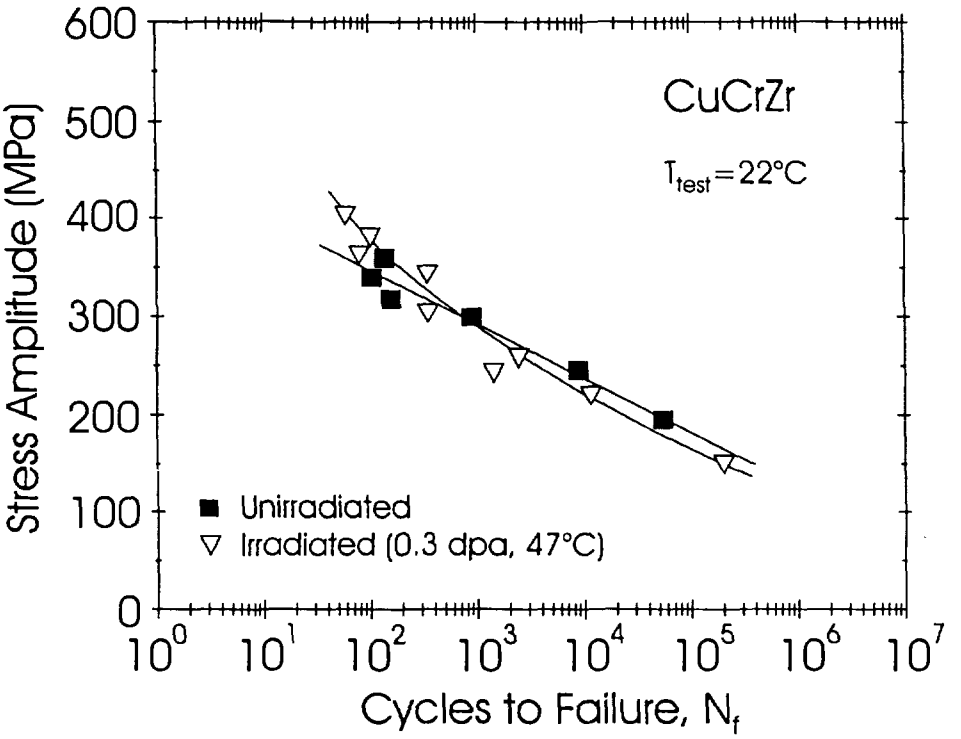

Figure 4. Fatigue life (N_f) as a function of stress amplitude for unirradiated and irradiated prime aged CuCrZr tested at room temperature in vacuum. Irradiation was carried out at ~47°C to a dose level of 0.3 dpa (NRT). All tests were carried out in the stress-controlled mode.

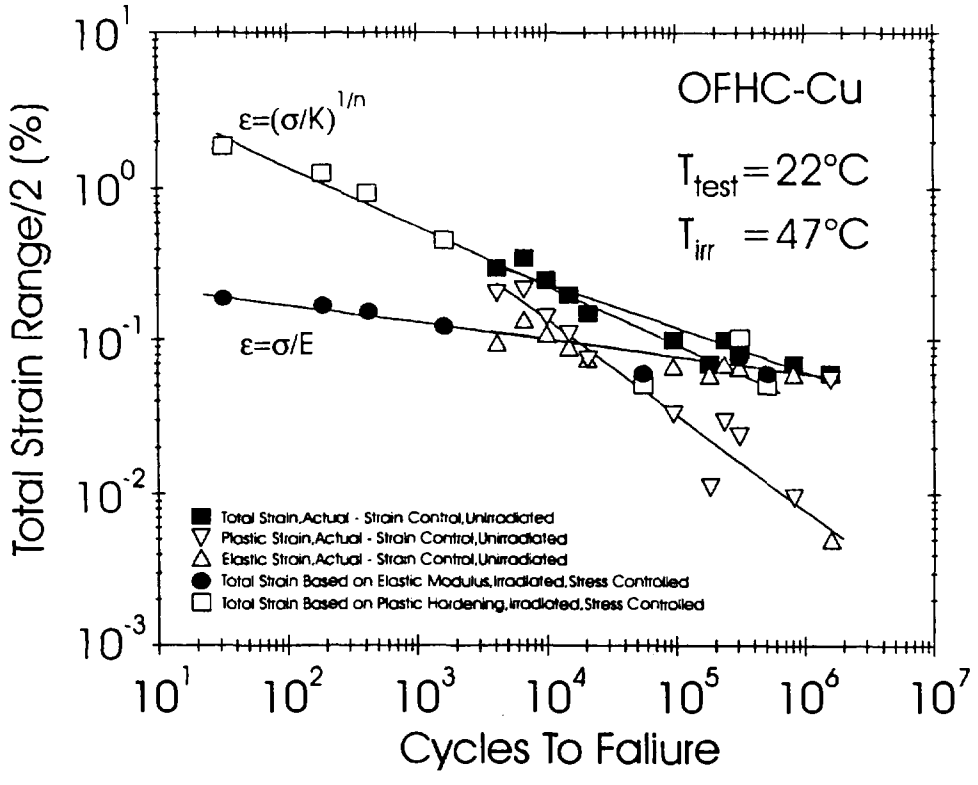

Figure 14. Fatigue life (N_f) as a function of the measured and calculated (from cyclic stress-strain curves) strains for the unirradiated and irradiated (at ~47°C) OFHC-copper tested at 22°C.

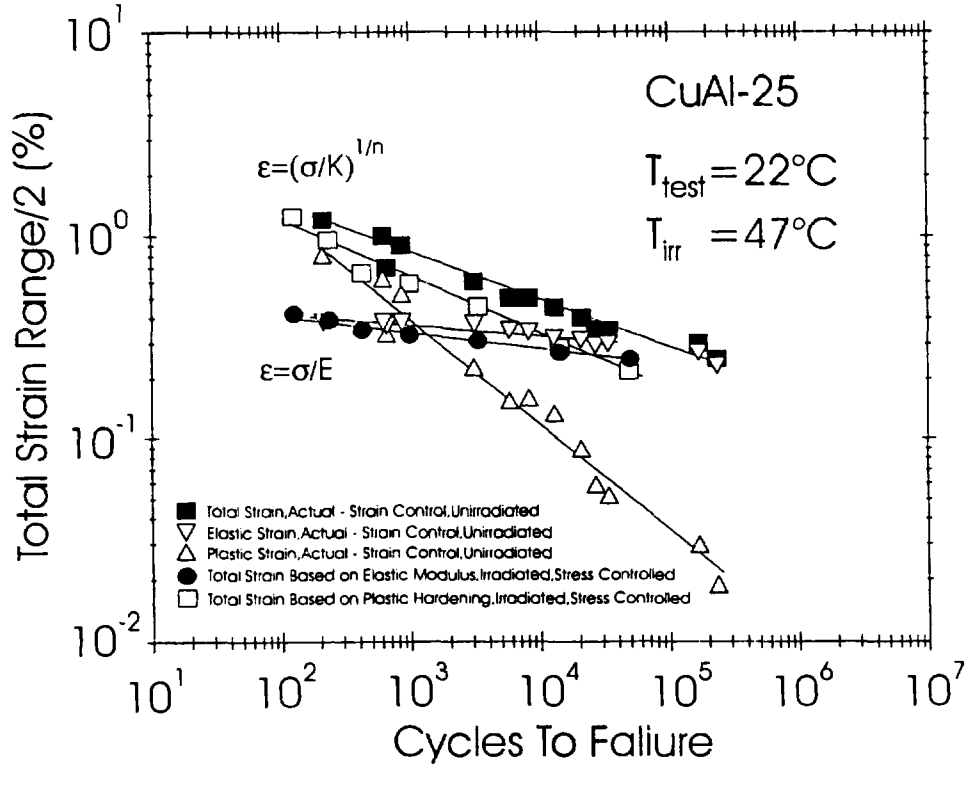

Figure 15. The same as in Figure 14, but for CuAl-25 irradiated at 47°C and tested at 22°C.

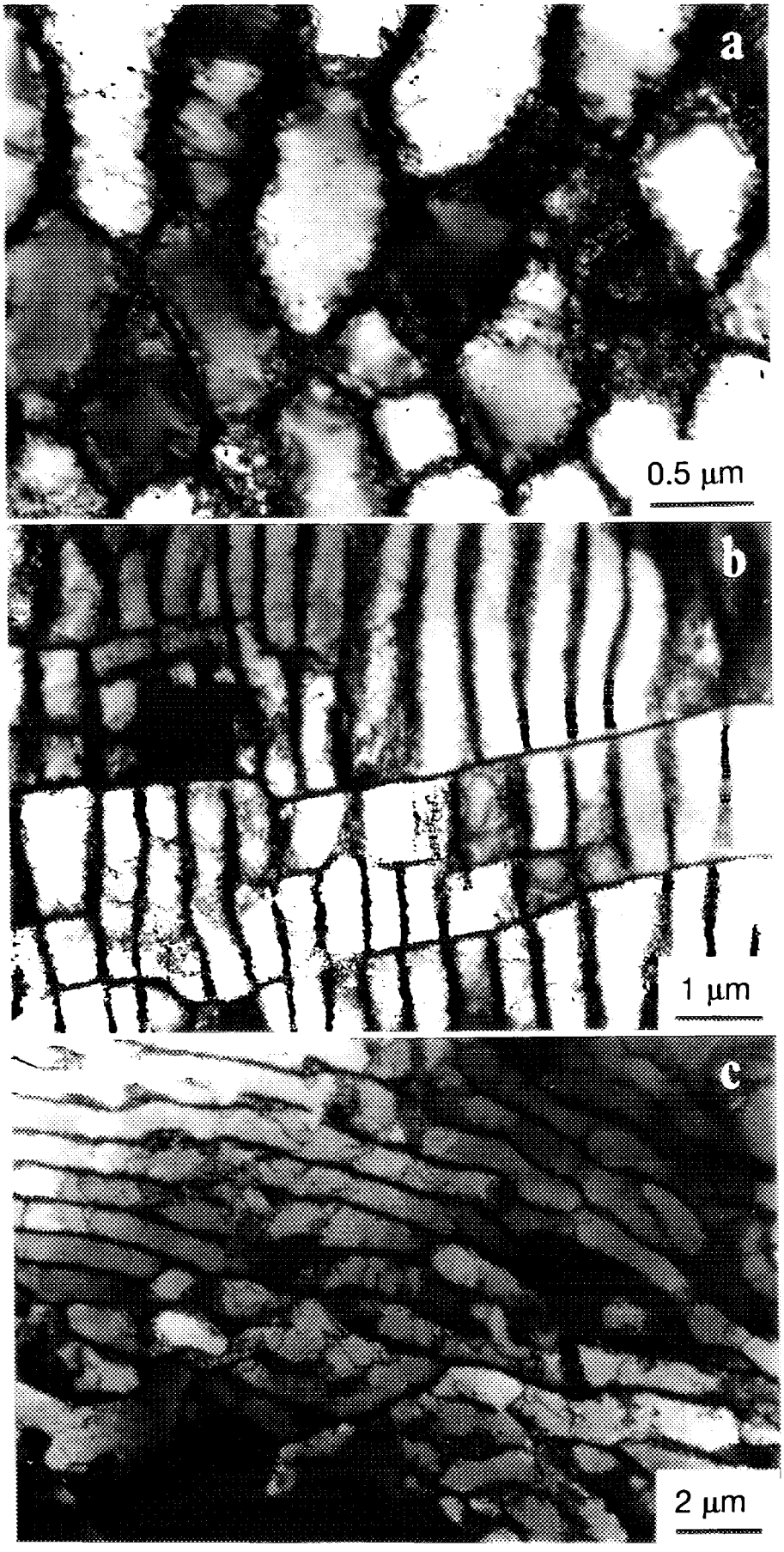

Figure 16. Post-fatigue microstructure of the unirradiated OFHC-Cu tested at room temperature showing formation of equiaxed and elongated cells: (a,b) 180 MPa, N_f = 1121, (c) 120 MPa, N_f = 21646.

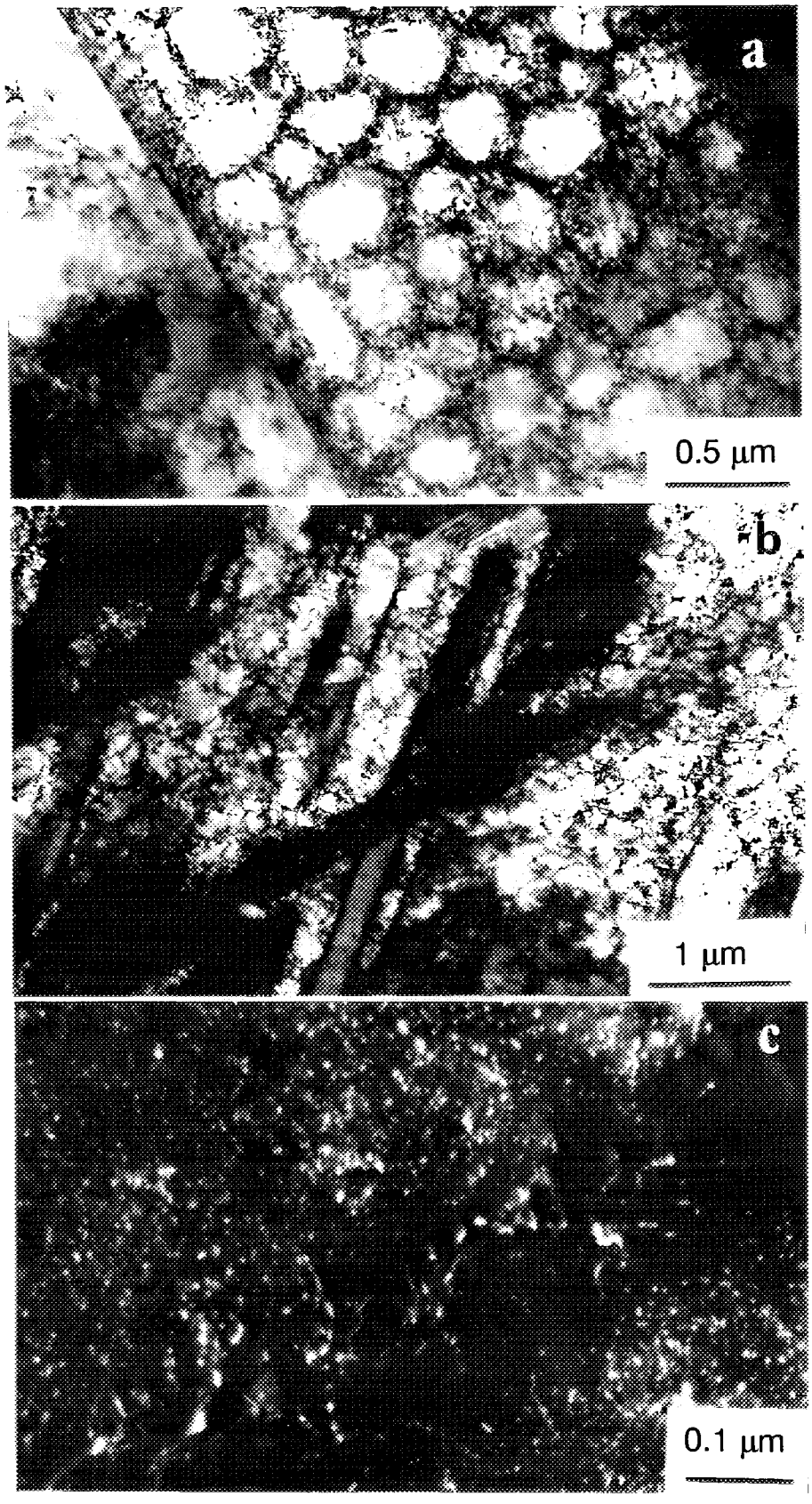

Figure 17. Post-fatigue microstructure of the OFHC-Cu irradiated at 47°C to 0.5 dpa and tested at room temperature at a stress amplitude of 250 MPa (N_f = 32) showing significant area to area variations: (a) small cells with loose dislocation walls, (b) slip bands, and (c) "cleared" channels. Note the lack of dislocation generation in the regions away from the cleared channel (c).

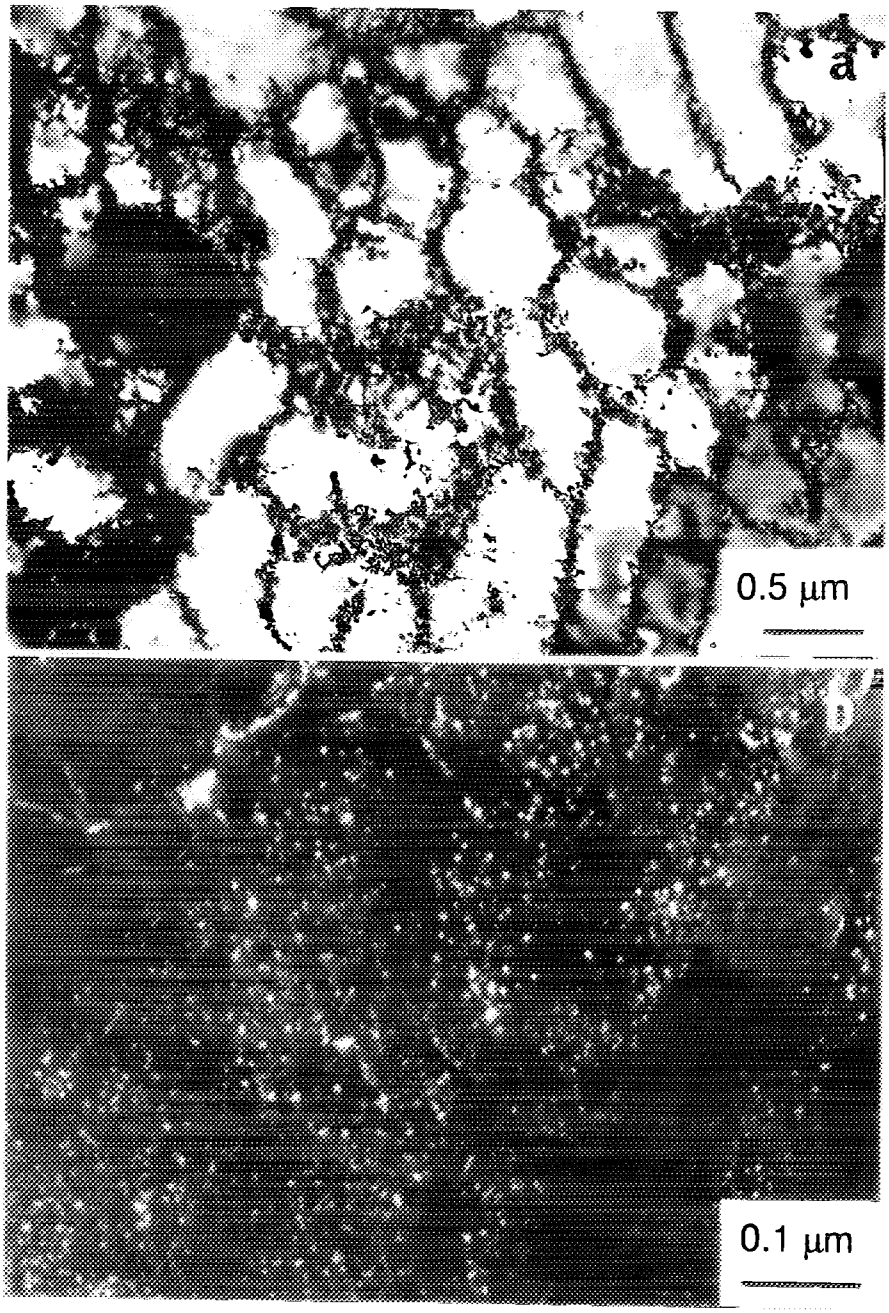

Figure 18. Same as in Fig. 17, but tested at a stress amplitude of 200 MPa (N_f = 424): (a) equiaxed and elongated cells and (b) cleared channels.

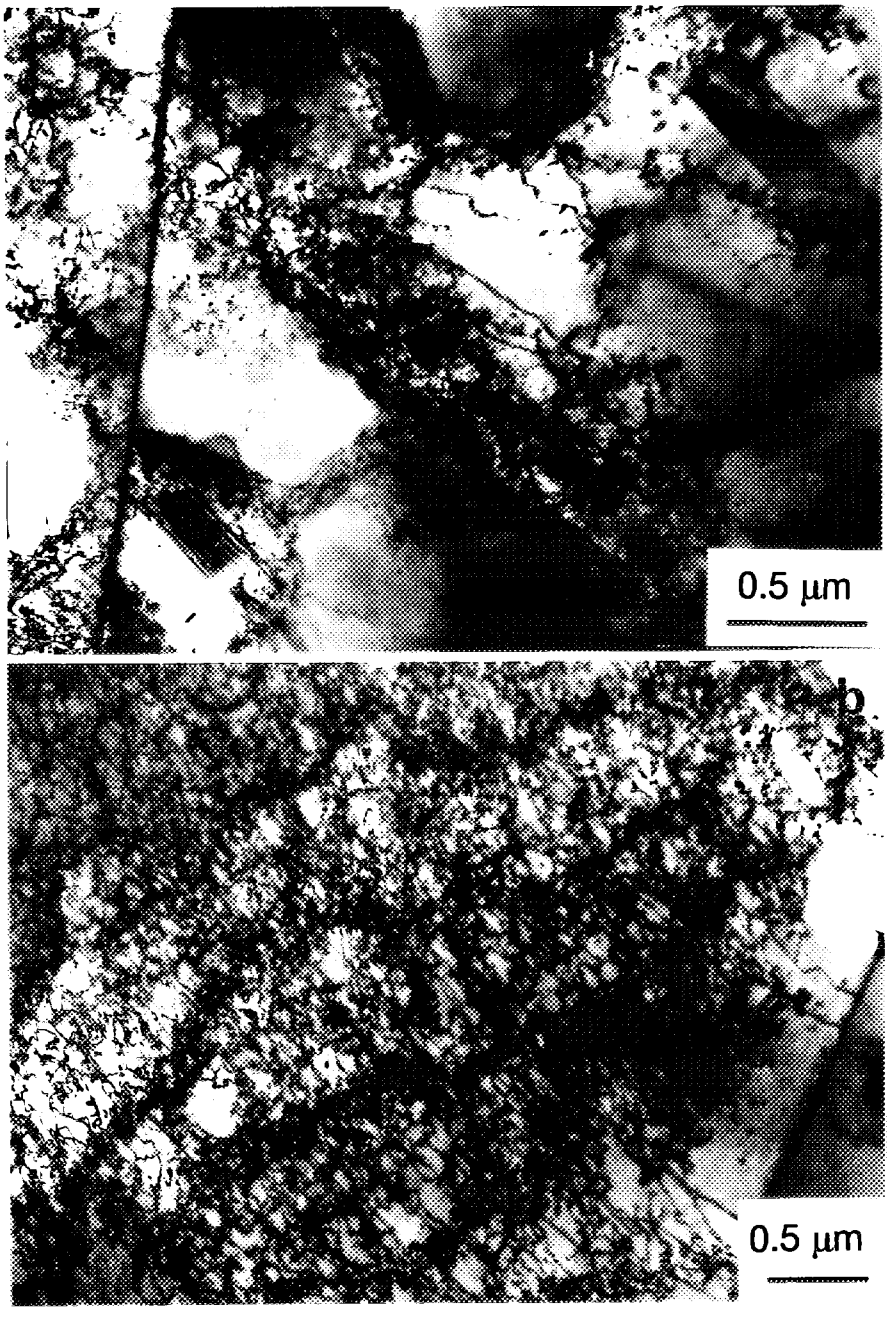

Figure 19. Same as in Fig. 17, but tested at a stress amplitude of 160 MPa (N_f = 1604): (a) tendency to form cells and (b) homogeneous distribution of dislocations.

Figure 20. Same as in Fig. 17, but tested at a stress amplitude of 80 Mpa (N_f = 56634) showing no indication of cell formation.

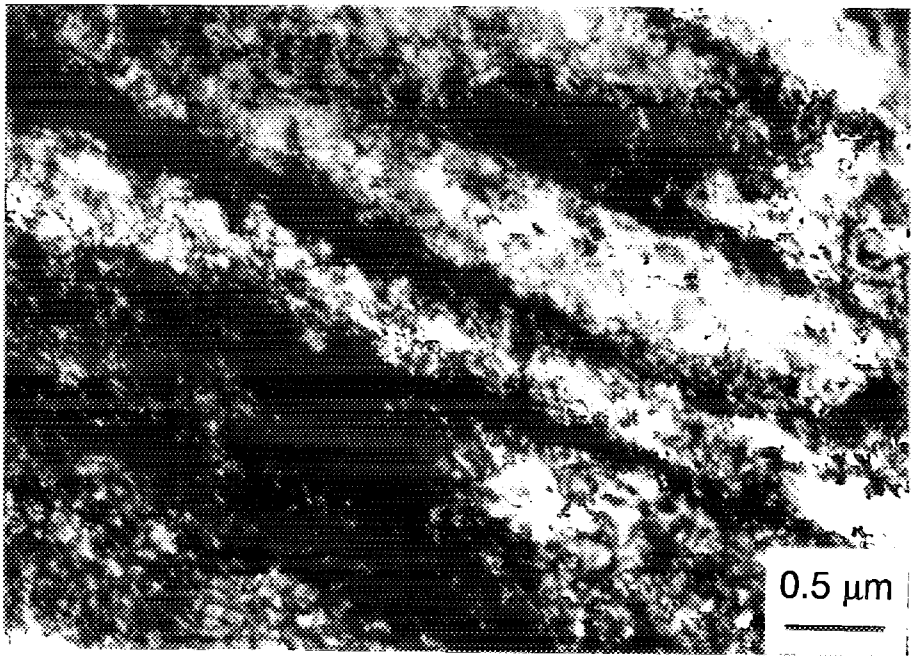

Figure 21. Same as in Fig. 17, but tested at a stress amplitude of 80 MPa (N_f = 515928) showing bands of dislocations.

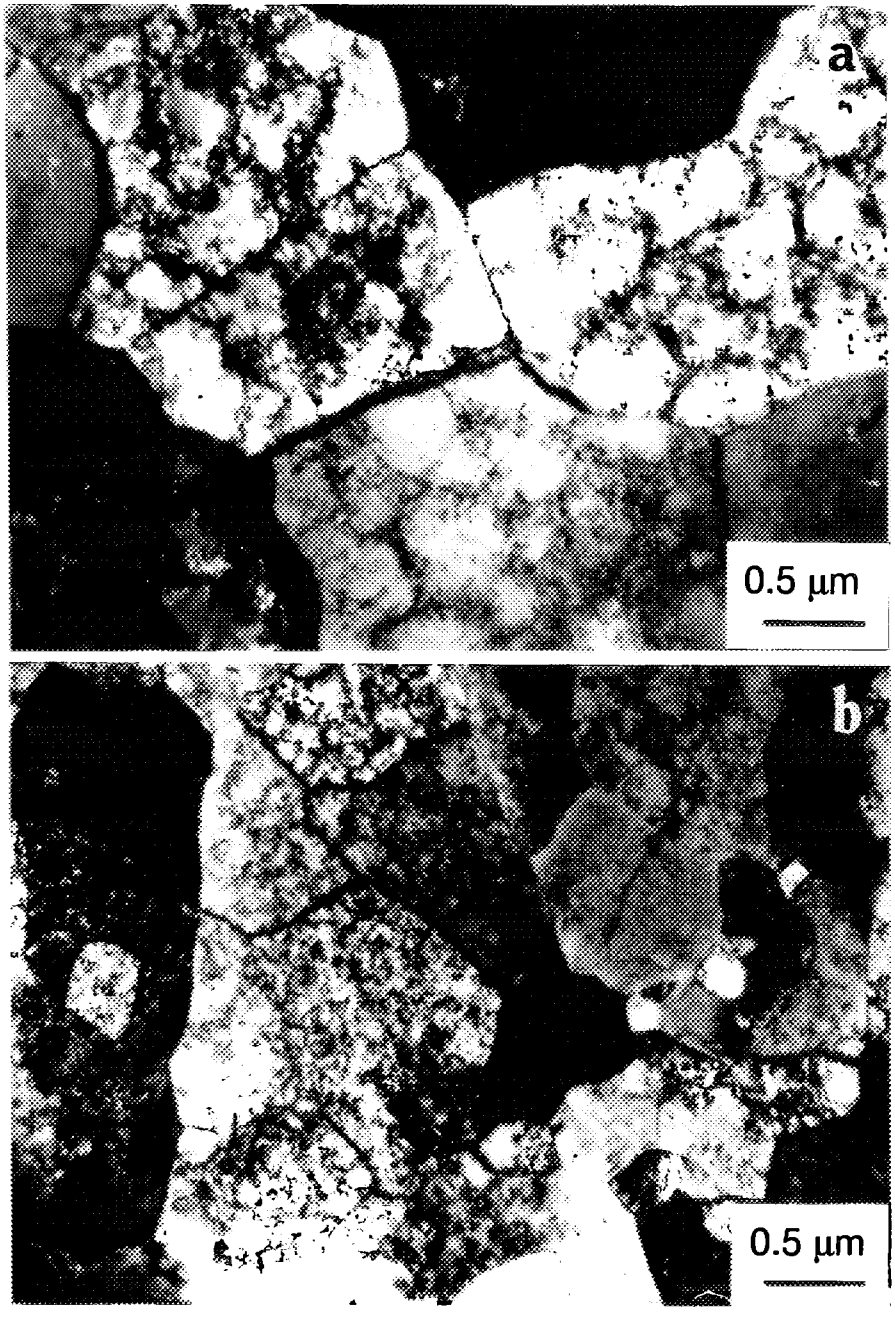

Figure 22. Post-fatigue microstucture of the unirradiated CuAl-25 alloy tested at room temperature at a stress amplitude of 440 MPa (N_f = 262): (a) small cells with loose dislocation walls and (b) rather homogeneous distribution of dislocations.

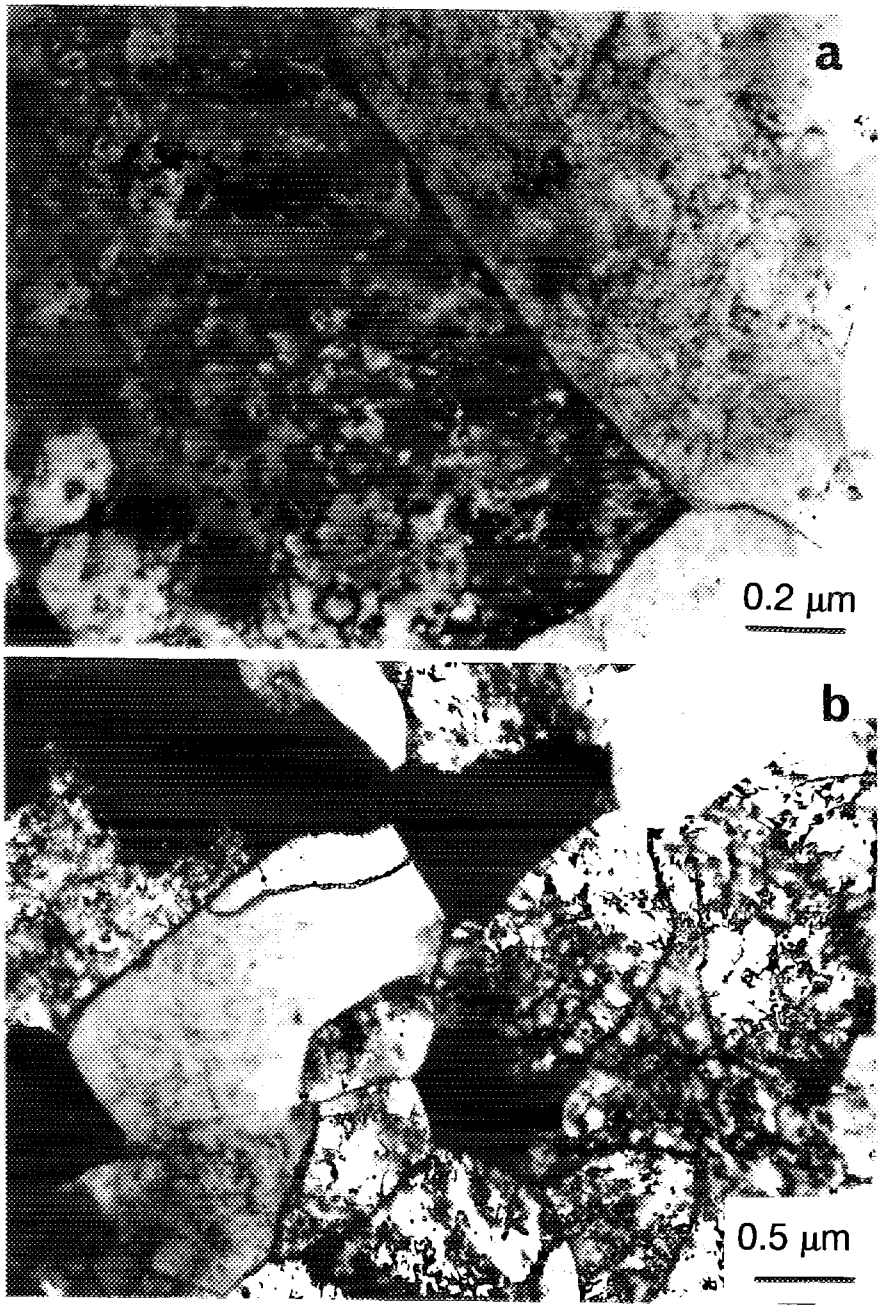

Figure 23. Same as in Fig. 22, but tested at a stress amplitude of 360 MPa (N_f = 2994) showing homogeneous distribution of dislocations at (a) low and (b) high magnification. Note, the lack of long-range dislocation transport and interaction.

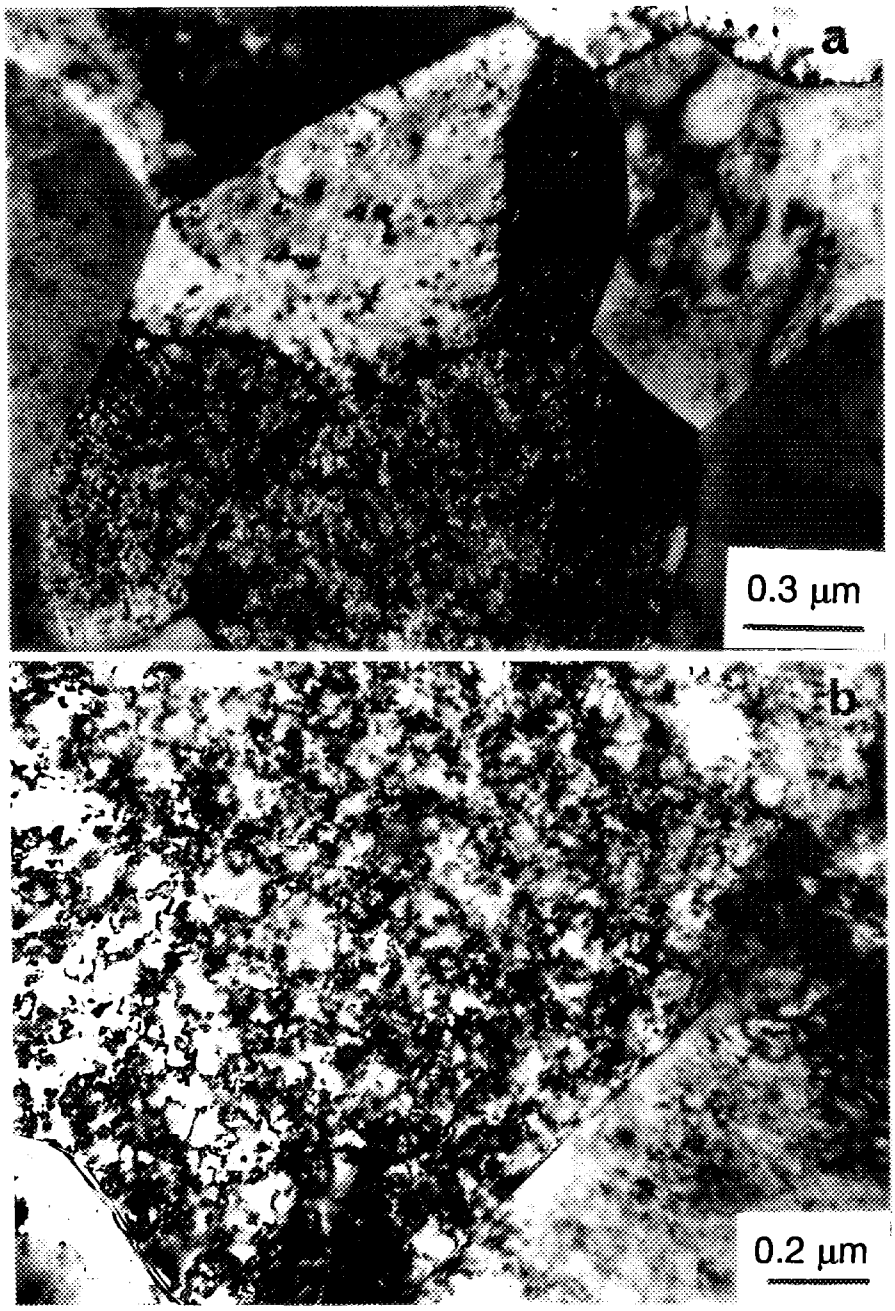

Figure 24. Post-fatigue microstructure of the irradiated (0.3 dpa, 47°C) CuAl-25 alloy tested at room temperature at a stress amplitude of (a) 540 MPa (N_f = 129) and (b) 320 MPa (N_f = 49506). At the stress amplitude of 320 MPa there appears to be no evidence of dislocation generation and migration.

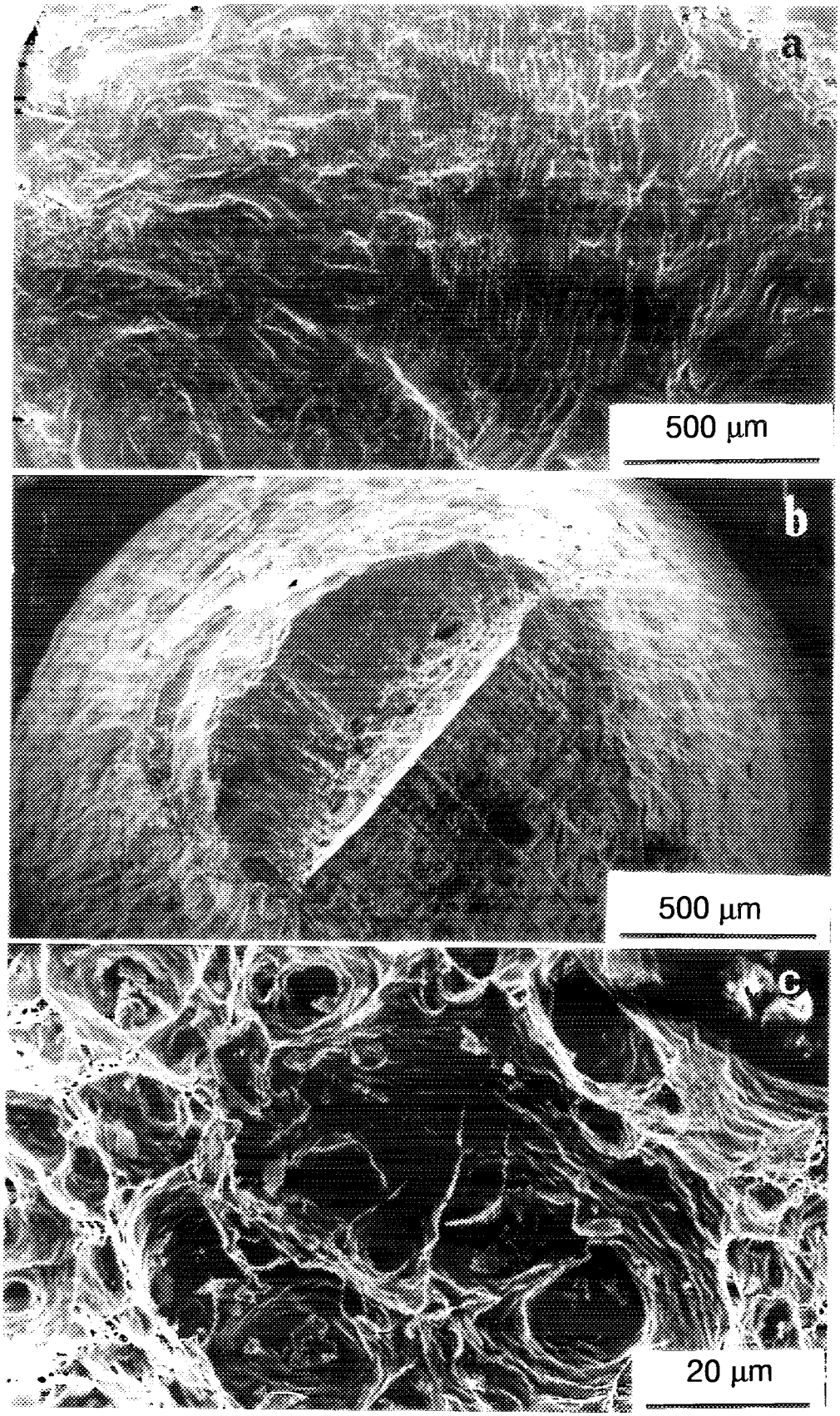

Figure 25. SEM fractographs of the fracture surfaces of fatigue tested OFHC-copper at 22°C in (a) unirradiated (N_f = 1121), (b) irradiated (47°C, 0.5 dpa, N_f = 32) conditions, and (c) same as (b), but at a higher magnification showng extensive deformation

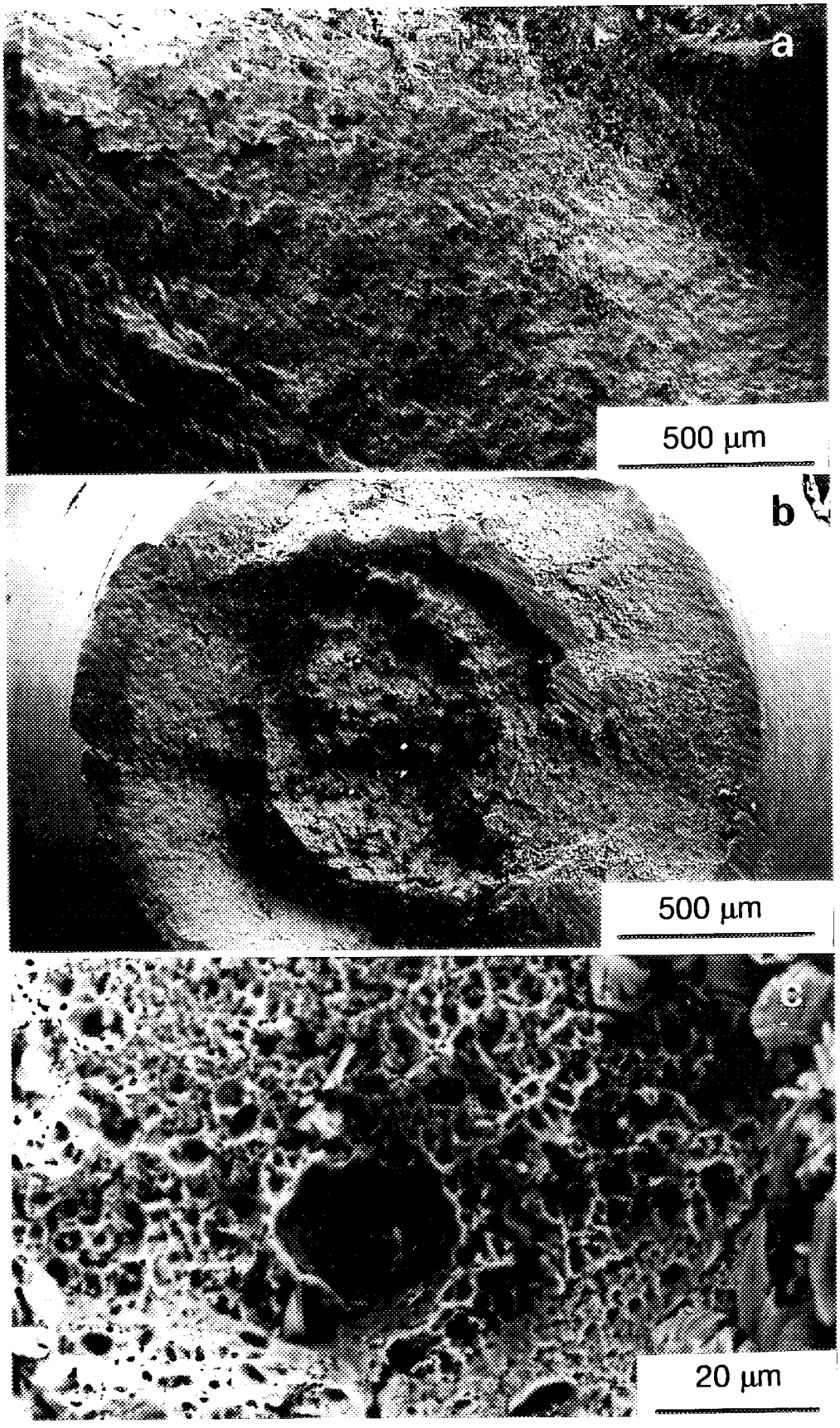

Figure 26. SEM fractographs of the fracture surfaces of fatigue tested CuAl-25 at 22°C in (a) unirradiated (N_f = 262), (b) irradiated (47°C, 0.3 dpa, N_f = 129) conditions, and (c) Same as (b), but at a higher magnification showing a large amount of plasticity-induced deformation voids.

Bibliographic Data Sheet **Risø-R-991(EN)**

Title and authors

Fatigue Performance of Copper and Copper alloys before and after Irradiation with Fission Neutrons

B.N. Singh, J.F. Stubbins and P. Toft

ISBN	ISSN
87-550-2313-4	0106-2840

Department or group	Date
Materials Research Department	May 1997

Groups own reg. number(s)	Project/contract No(s)

Pages	Tables	Illustrations	References
42	4	26	10

Abstract (max. 2000 characters)

The fatigue performance of pure copper of the oxygen free, high conductivity (OFHC) grade and two copper alloys (CuCrZr and CuAl-25) was investigated. Mechanical testing and microstructural analysis were carried out to establish the fatigue life of these materials in the unirradiated and irradiated states. The present report provides the first information on the ability of these copper alloys to perform under cyclic loading conditions when they have undergone significant irradiation exposure. Fatigue specimens of OFHC-Cu, CuCrZr and CuAl-25 were irradiated with fission neutrons in the DR-3 reactor at Risø with a flux of ~2.5 × 10^{17} n/m^2s (E > 1 MeV) to fluence levels of 1.5 - 2.5 × 10^{24} n/m^2s (E >1 MeV) at ~47 and 100°C. Specimens irradiated at 47°C were fatigue tested at 22°C, whereas those irradiated at 100°C were tested at the irradiation temperature.

The major conclusion of the present work is that although irradiation causes significant hardening of copper and copper alloys, it does not appear to be a problem for the fatigue life of these materials. In fact, the present experimental results clearly demonstrate that the fatigue performance of the irradiated CuAl-25 alloy is considerably better in the irradiated than that in the unirradiated state tested both at 22 and 100°C. This improvement, however, is not so significant in the case of the irradiated OFHC-copper and CuCrZr alloy tested at 22°C.These conclusions are supported by the microstructural observations and cyclic hardening experiments.

Descriptors INIS/EDB

COPPER ALLOYS; FATIGUE; FISSION NEUTRONS; ITER TOKAMAK; MECHANICAL TESTS; MICROSTRUCTURE; PHYSICAL RADIATION EFFECTS; RADIATION HARDENING; TEMPERATURE RANGE 0273-0400 K; THERMONUCLEAR REACTOR MATERIALS

Available on request from Information Service Department, Risø National Laboratory, (Afdelingen for Informationsservice, Forskningscenter Risø), P.O.Box 49, DK-4000 Roskilde, Denmark. Telephone +45 4677 4677, ext. 4004/4005, Telex 43 116, Telefax +45 4677 4013

RISØ

Objective

Risø National Laboratory carries out research within science and technology, providing Danish society with new opportunities for technological development. The research aims at strengthening Danish industry and reducing the adverse impact on the environment of the industrial, energy and agricultural sectors.
Risø has a special responsibility for the consolidation of the knowledge base for consultancy on nuclear affairs.

Research profile

Risø performs long-term research of relevance to Danish society. This research is part of a range of Danish and international research programmes and similar collaborative ventures. Risø undertakes research, development and consultancy projects for the authorities and industry. The main emphasis is on basic research and participation in strategic collaborative research ventures. Research is carried out within the following programme areas:

Industrial materials
New functional materials
Optics and sensor systems
Plant production and ecology
Systems analysis
Wind energy and atmospheric processes
Nuclear safety

Risø-R-991(EN)
ISBN 87-550-2313-4
ISSN 0106-2840

Copies of this publication
are available from
Risø National Laboratory
Information Service Department
P.O. Box 49
DK-4000 Roskilde
Denmark
Telephone +45 4677 4677,
ext. 4004/4005
e-mail: risoe@risoe.dk
Fax +45 4677 4013
http://www.risoe.dk

Product, target groups and collaboration

Risø's product is knowledge and technological development generated by high-quality research. The target groups are industry, the authorities and the research community. Risø collaborates with universities, research institutes, institutes of technology and businesses. A strong emphasis is placed on the education of young researchers through Ph.D. and post-doctoral programmes.

Key figures

Risø has 960 employees, including 360 researchers and 100 Ph.D. candidates and post-doctoral personnel. Risø's 1997 budget is DKK 485 m, of which DKK 223 m is income from programme research and contract work. The balance is funded by Government grant.